ISCI, Volume *17*

Supplemental Information

Vitamin D/Vitamin D Receptor Signaling Is Required for Normal Development and Function of Group 3 Innate Lymphoid Cells in the Gut

Lei He, Min Zhou, and Yan Chun Li

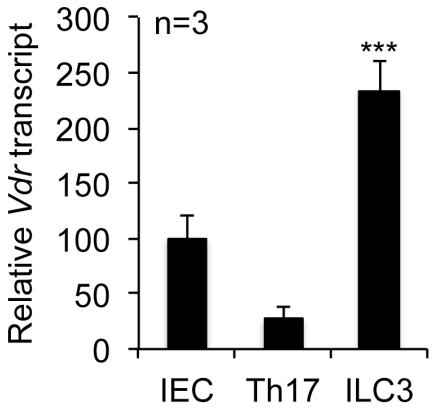

Figure S1. High level VDR expression in ILC3, Related to Figure 1.
Real time RT-PCR quantification of *Vdr* transcript in purified intestinal epithelial cells, and sorted T_H17 cells and ILC3. Data are represented as mean ± SEM.

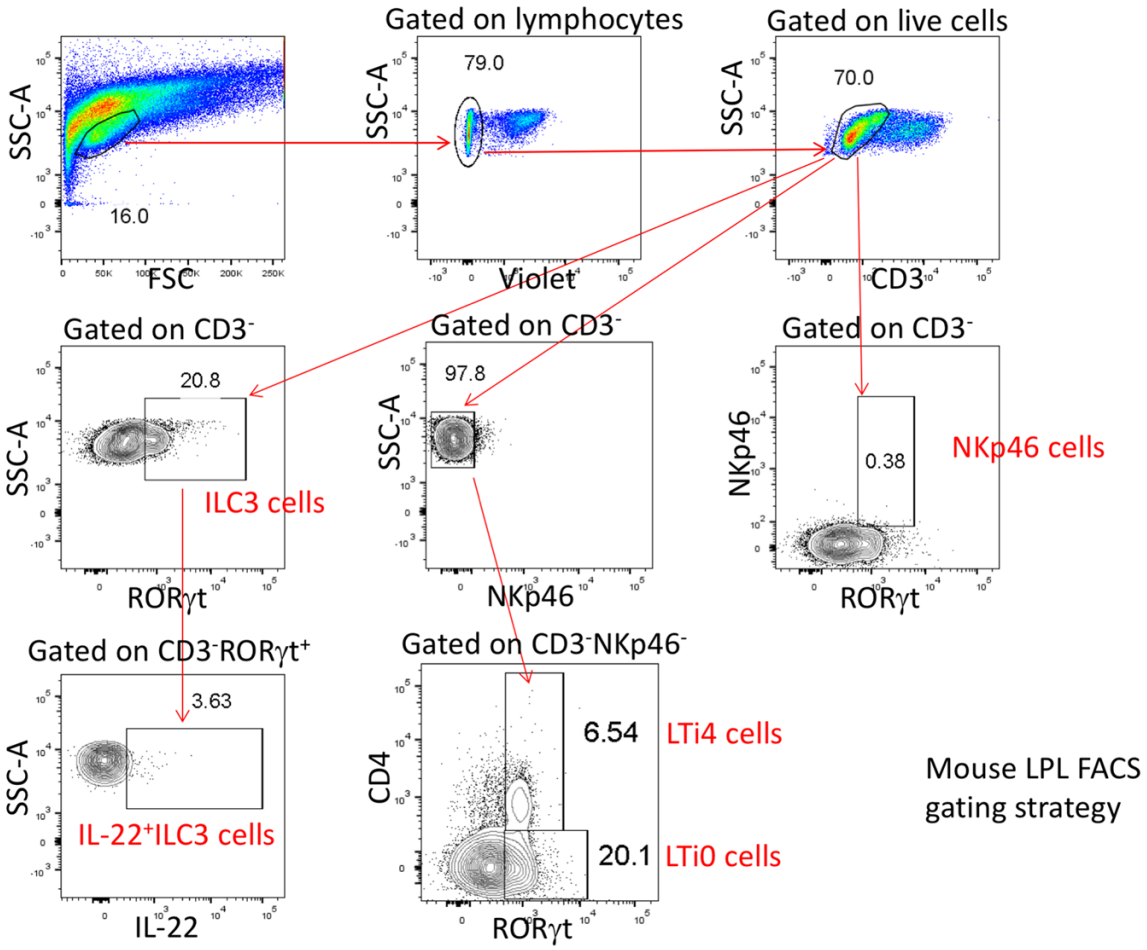

Figure S2. Flow cytometry gating strategies for FACS analyses of gut ILC3 and its sub-populations from lamina propria cells, Related to Figure 1.

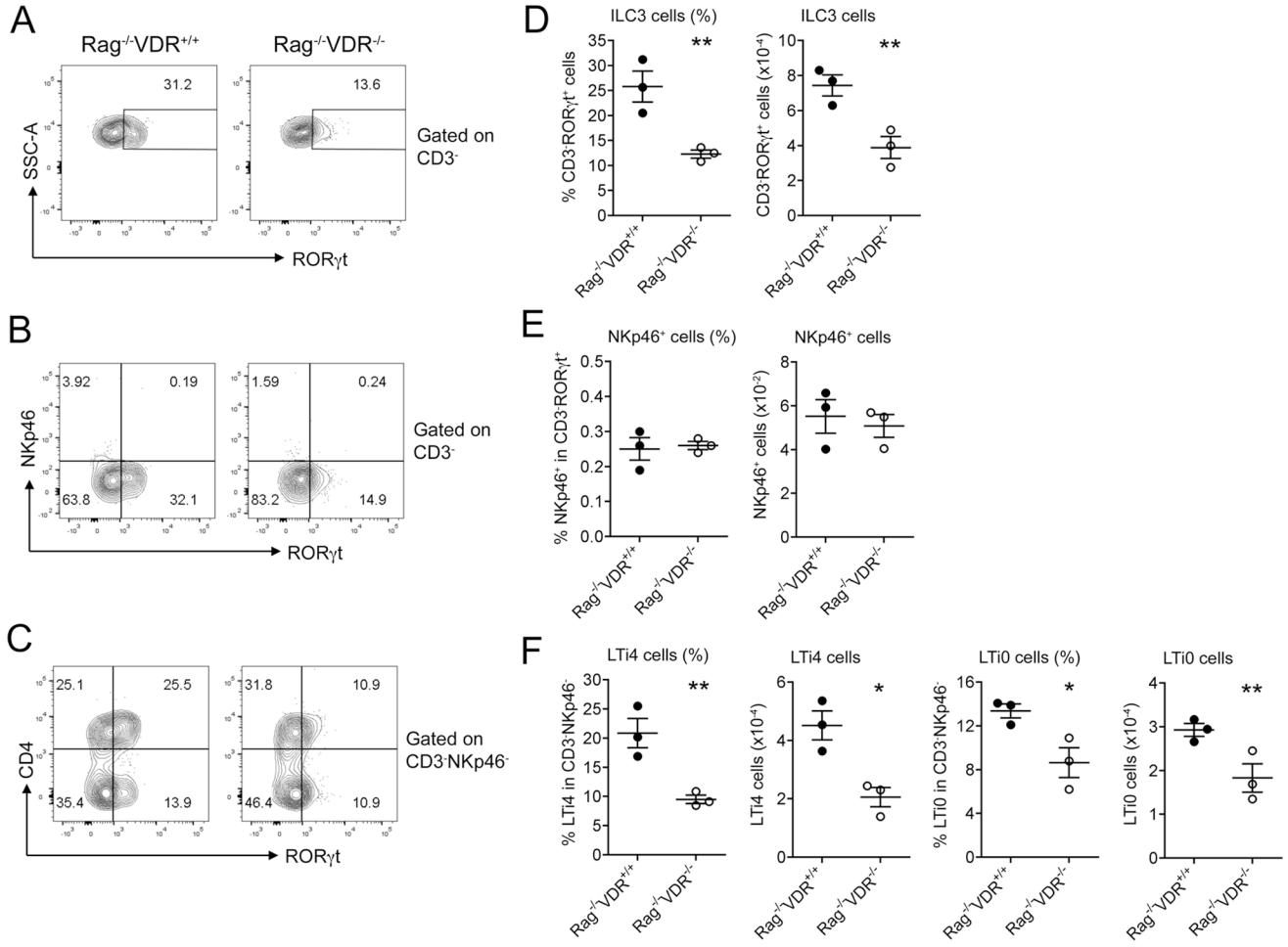

Figure S3. Effects of VDR deletion on gut ILC3 development is independent of T and B cells, Related to Figure 1.

Colonic lamina propria cells were isolated from Rag1$^{-/-}$VDR$^{+/+}$ and Rag1$^{-/-}$VDR$^{-/-}$ mice, and the cells were analyzed by FACS for ILC3 populations.

(A-C) Representative FACS plots for analysis of RORγt^{+}ILC3 (A), NKp46^{+} cells (B) and LTi4 and LTi0 cells (C) in Rag1$^{-/-}$VDR$^{+/+}$ and Rag1$^{-/-}$VDR$^{-/-}$ mice at steady state.

(D-F) Quantitation based on FACS data of RORγt^{+}ILC3 (D), NKp46^{+} cells (E) and LTi4 and LTi0 cells (F) in Rag1$^{-/-}$VDR$^{+/+}$ and Rag1$^{-/-}$VDR$^{-/-}$ mice.

The data were presented as percentage of the gated population and absolute cell number. *P<0.05; **P<0.01; ***P<0.001. n=3 each genotype. Data are represented as mean ± SEM.

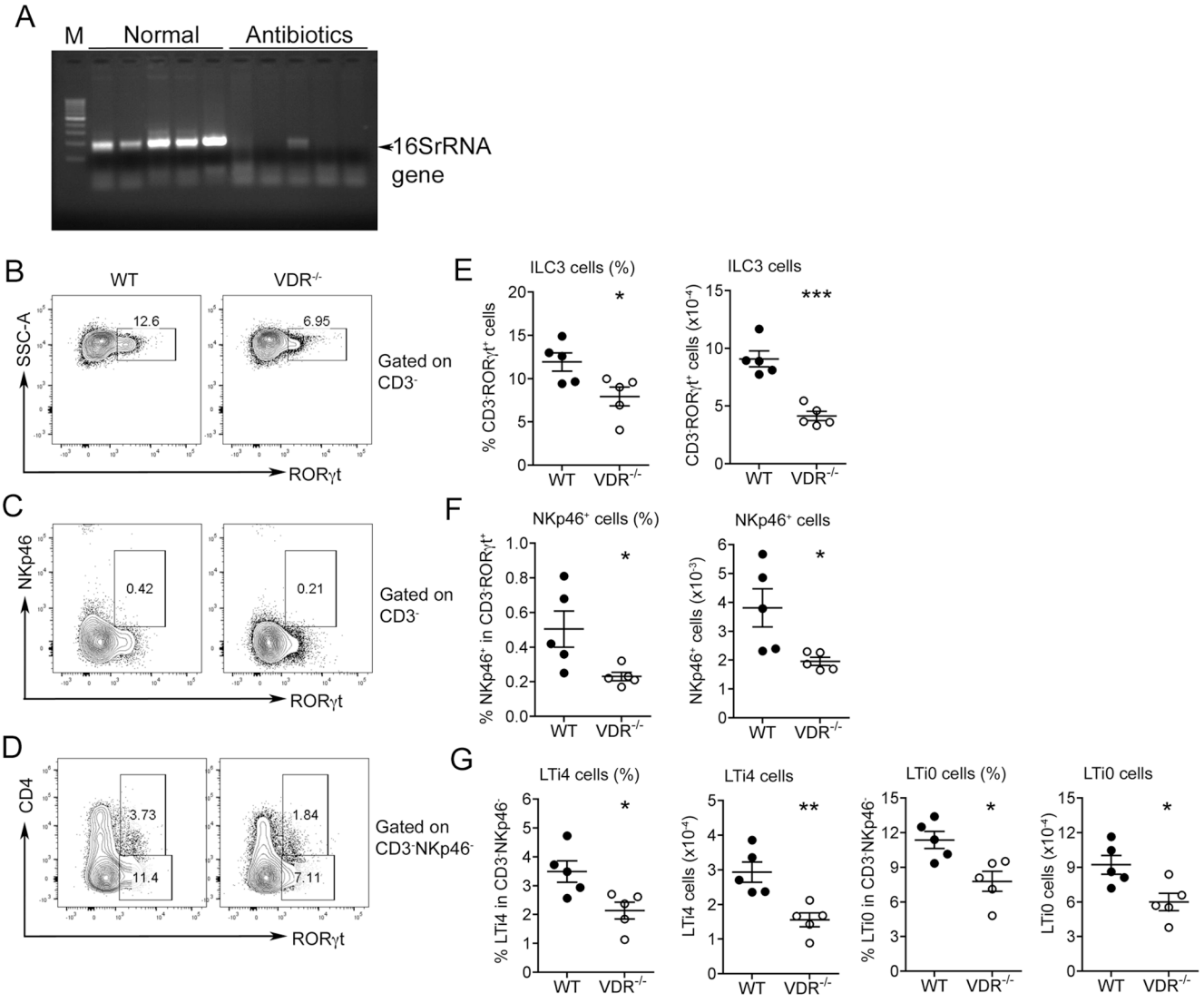

Figure S4. Effects of VDR deletion on gut ILC3 development is independent of gut commensal bacteria, Related to Figure 1.

Colonic lamina propria cells were isolated from WT and VDR$^{-/-}$ mice treated with the antibiotic cocktail for 4 weeks, and the cells were analyzed by FACS for ILC3 populations.

(A) PCR amplification of 16S rRNA gene from DNA purified from fecal pellets. Each lane contains DNA from two fecal pellets amplified by 25 PCR cycles. Each lane represents one mouse.

(B-D) Representative FACS plots for analysis of RORγt^{+}ILC3 (B), NKp46^{+} cells (C) and LTi4 and LTi0 cells (D).

(E-G) Quantitation based on FACS data of RORγt^{+}ILC3 (E), NKp46^{+} cells (F) and LTi4 and LTi0 cells (G).

The data were presented as percentage of the gated population and absolute cell number. *P<0.05; **P<0.01; ***P<0.001. n=5 each genotype. Data are represented as mean ± SEM.

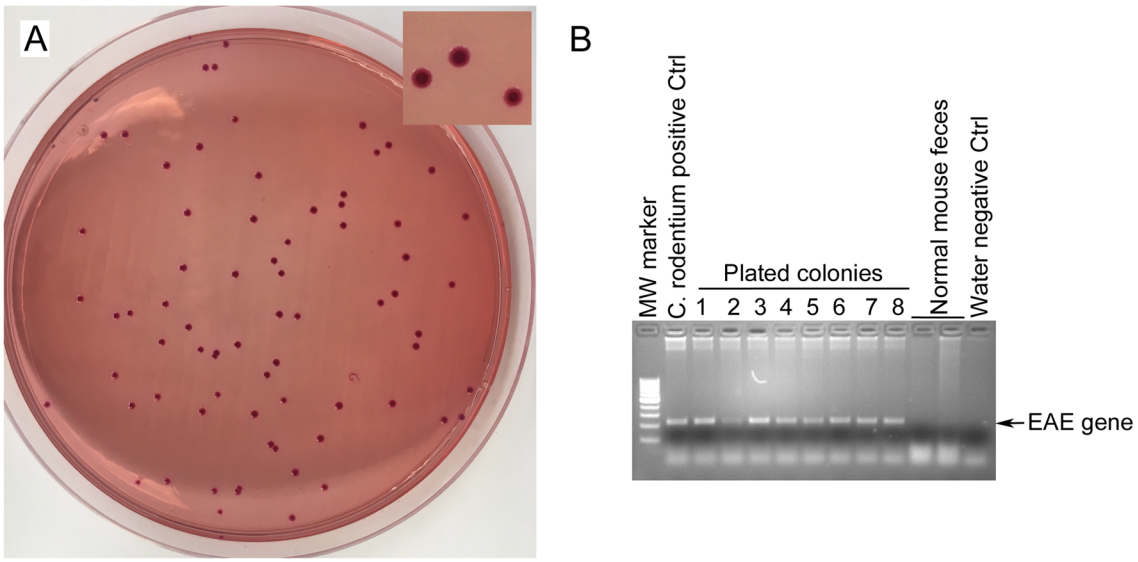

Figure S5. Quantitation of fecal *C. rodentium*, Related to Figure 2.
(A) Representative MacConkey agar plate showing *C. rodentium* colonies, whose distinctive morphology is characterized by a pink center with white rim. *Inset* shows an enlarged image of the colonies.
(B) PCR amplification of the *eae* gene from 8 randomly picked colonies. The *eae* gene was undetectable from normal, uninfected mouse feces.

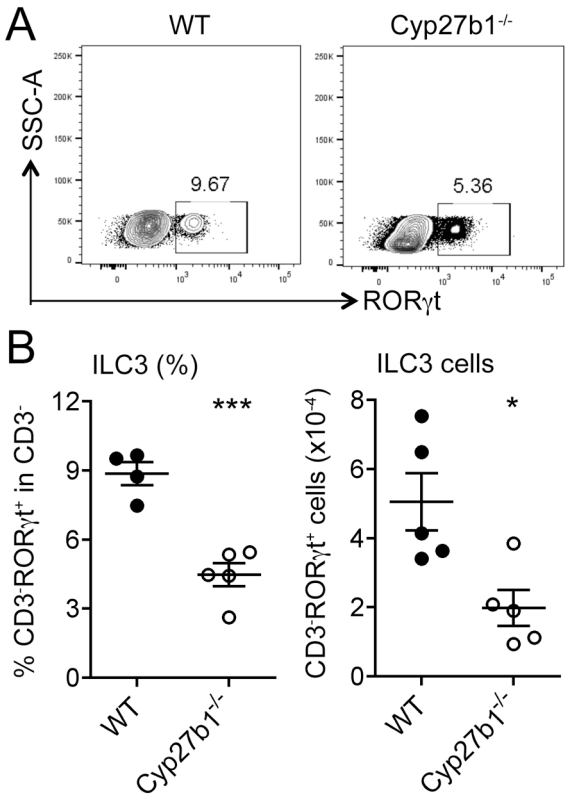

Figure S6. 1,25(OH)$_2$D$_3$ deficiency impairs gut ILC3 development, Related to Figure 3.
Colonic lamina propria cells were isolated from WT and Cyp27b1$^{-/-}$ mice, and the cells were analyzed by FACS for ILC3 populations.
(A) Representative FACS plots for analysis of RORγt$^+$ILC3;
(B) Quantitation of RORγt$^+$ILC3 in percentage and absolute cell number. *P<0.05; ***P<0.001. n=4-5 each genotype.

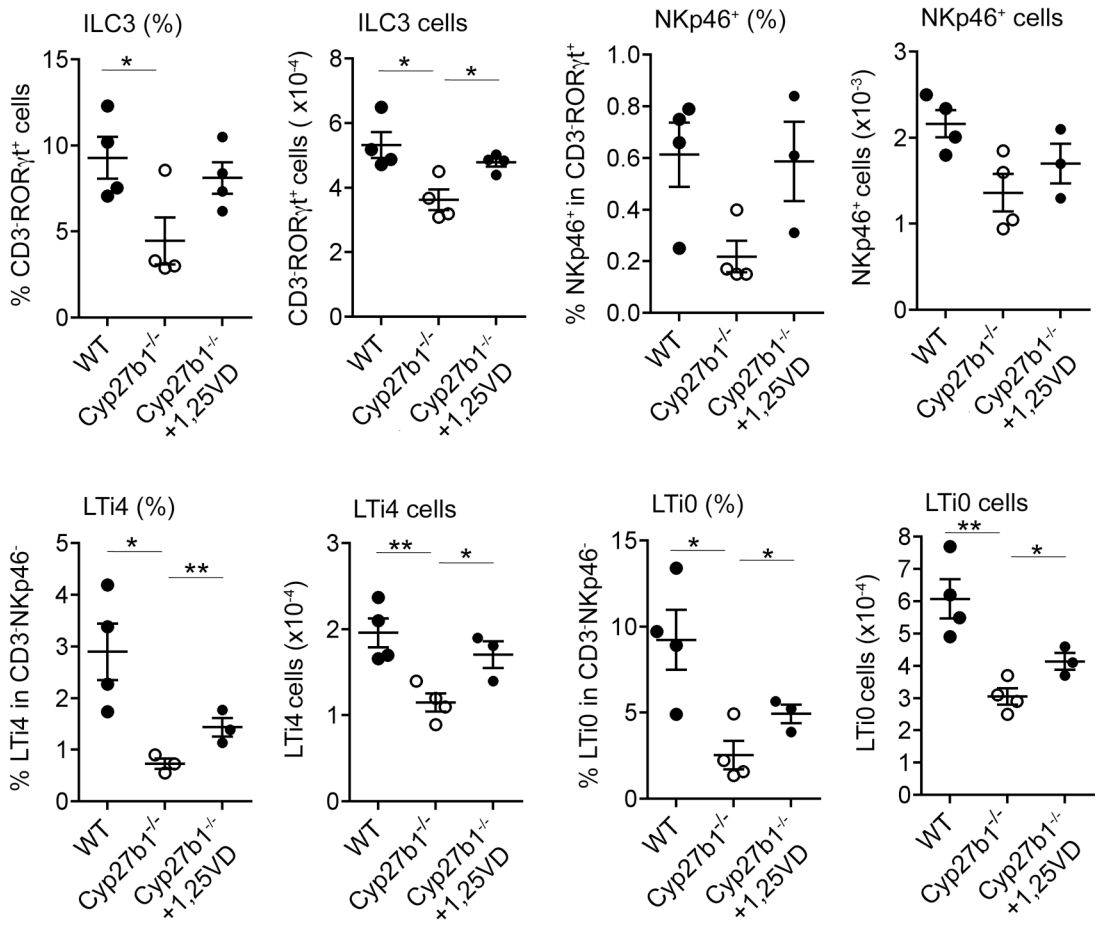

Figure S7. Reconstitution of Cyp27b1$^{-/-}$ mice with 1,25(OH)$_2$D$_3$ restores gut ILC3 populations, Related to Figure 3.

Colonic LP cells were isolated from WT, Cyp27b1$^{-/-}$ or Cyp27b1$^{-/-}$ mice treated with 1,25(OH)$_2$D$_3$ for one week, and gut ILC3 populations were quantified by FACS analyses. Shown are quantitation of RORγt$^+$ILC3, NKp46$^+$ cells, and LTi4 and LTi0 cells in percentage and absolute cell number. *P<0.05; **P<0.01; ***P<0.001. n=3-4 each group. Data are represented as mean ± SEM.

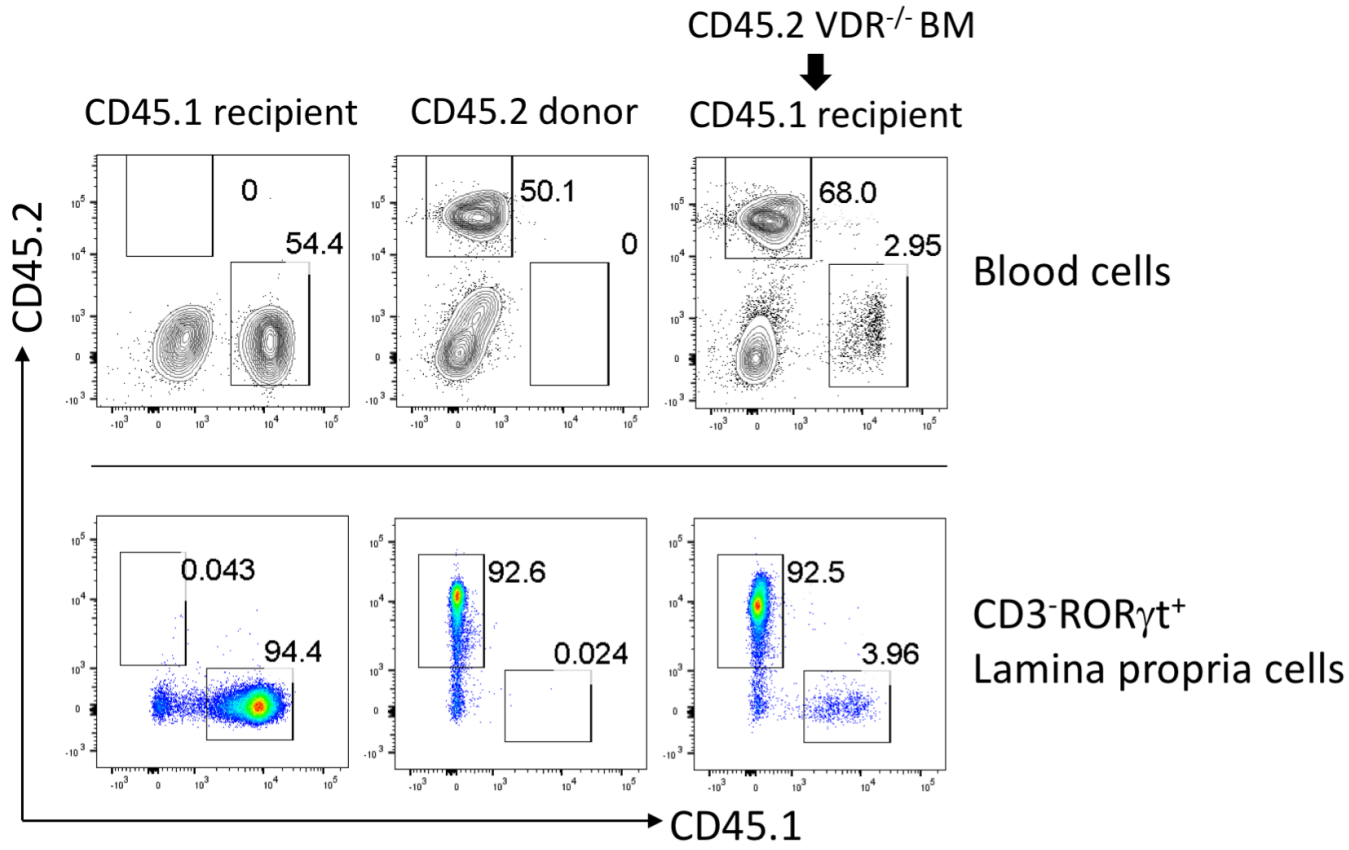

Figure S8. Validation of bone marrow transplantation, Related to Figure 5.
Bone marrow cells isolated from CD45.2 VDR-/- mice were transplanted to lethally irradiated CD45.1 recipient mice. Eight weeks later, blood and colonic lamina propria cells were analyzed by FACS. Note after transplantation the blood cells and colonic $CD3^{-}ROR\gamma t^{+}$ cells of the CD45.1 recipients had become CD45.2 positive.

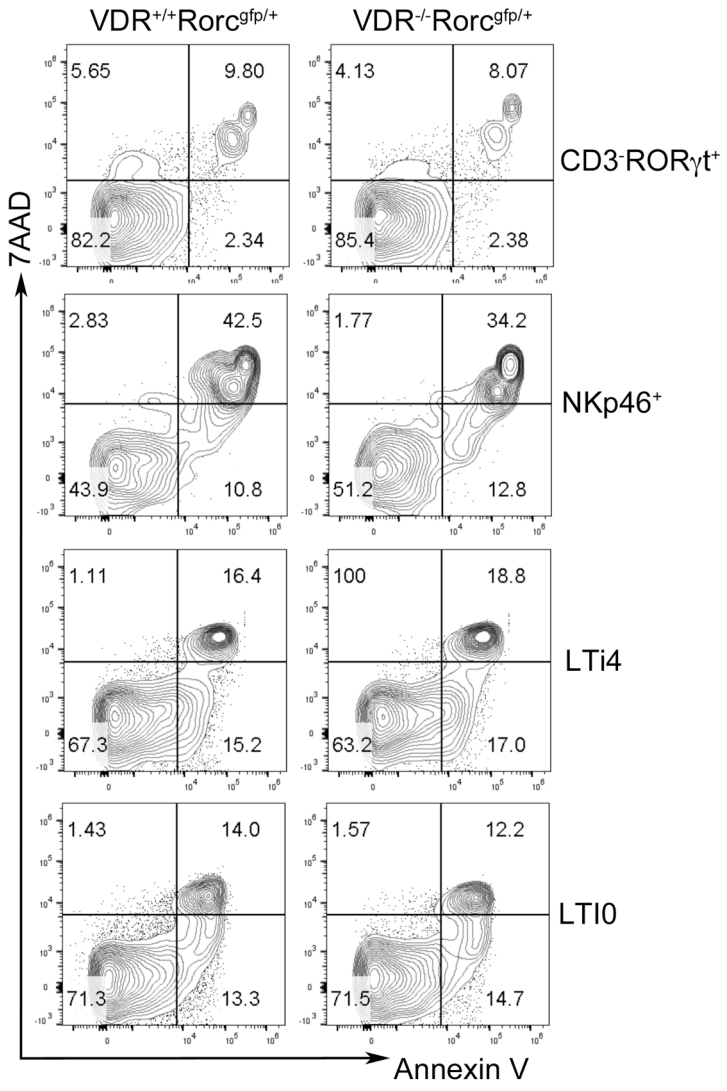

Figure S9. Effects of VDR deletion on gut ILC3 development is independent of ILC3 apoptosis, Related to Figure 6.

Colonic LP cells were isolated from VDR$^{+/+}$Rorc$^{gfp/+}$ and VDR$^{-/-}$Rorc$^{gfp/+}$ mice at steady state, the cells were analyzed for 7AAD and annexin V levels in ILC3 populations. Shown are representative FACS plots for analyses of RORγt^{+}ILC3, NKp46^{+} cells, and LTi4 and LTi0 cells.

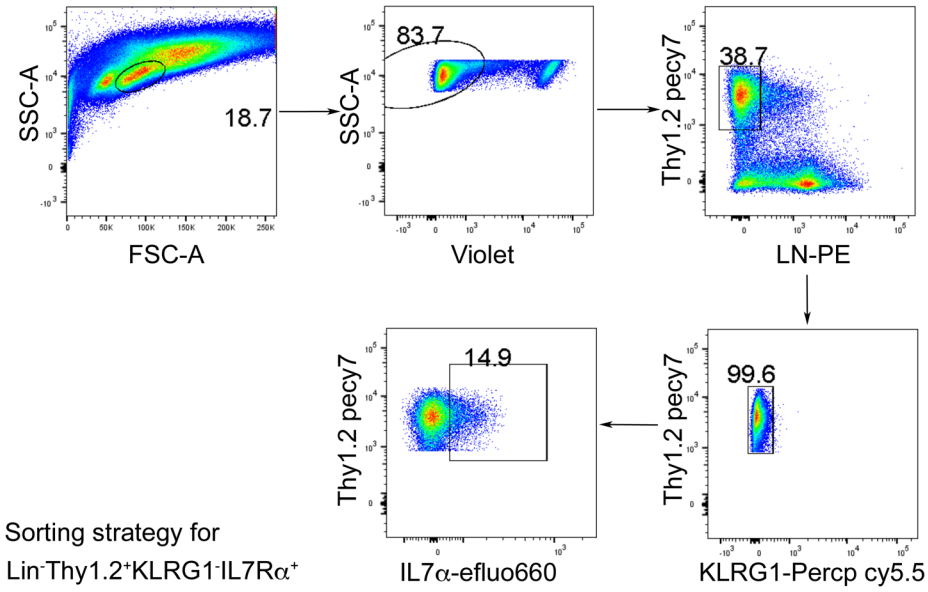

Figure S10. Sorting strategy for Lin$^-$ Thy1.2^{hi}KLRG1$^-$IL-7Rα$^+$ cells from colonic lamina propria cells that were isolated from Rag1$^{-/-}$ mice, Related to Figure 7.

Transparent Methods

Animals

$VDR^{-/-}$ mice were described previously (Li et al., 1997), and $Cyp27b1^{-/-}$ mice that carry a genetic deletion in the 1α-hydroxylase gene (Panda et al., 2001) were obtained from Dr. David Goltzman (McGill University). The $VDR^{-/-}$ and $Cyp27b1^{-/-}$ colonies were maintained on the high calcium/high lactose rescue diet as reported (Li et al., 1998). $VDR^{flox/flox}$ with LoxP sites flanking exon 4 of the *Vdr* gene were reported previously (Chen et al., 2011; He et al., 2018). $Rag1^{-/-}$ mice (Stock #: 002216) that have no mature T and B lymphocytes (Mombaerts et al., 1992), RORγt-EGFP mice ($Rorc^{gfp/+}$, Stock # 007572) that carry EGFP knock-in in the RORγt gene so that RORγt^{+} cells are GFP-positive, and RORγt-Cre transgenic mice (Stock # 022791) that express the Cre recombinase in RORγt-positive cells, were all obtained from Jackson Laboratory. $VDR^{flox/flox}$;RORγt-Cre and $VDR^{-/-}$;$Rag1^{-/-}$ mice were generated by crossing two corresponding strains of mice, respectively. In all studies 6-8 week old mice, both male and female, were used. All animal study protocols were approved by the Institutional Animal Care and Use Committee at the University of Chicago.

Citrobactor rodentium infection

C. rodentium bacteria (Strain DBS100, ATCC 51549) were grown in LB medium at 37°C. Mouse *C. rodentium* infection was carried out based on a method described previously (Koroleva et al., 2015). Mice were orally gavaged with *C. rodentium* at $1x10^{10}$ CFU/mouse suspended in 200 μl PBS for survival studies. For experiments examining ILC3 response, mice were gavaged with *C. rodentium* at $5x10^{9}$ CFU/mouse and killed day 4 or 5. Body weight and death were recorded daily. Feces were collected daily and stored at -80°C for later analyses. To quantify fecal bacteria, feces were weighed and then homogenized in sterile PBS containing 20% glycerol. Serially diluted homogenates were plated on Difco-MacConkey agar (BD Bioscience) plates (Bouladoux et al., 2017). *C. rodentium* colonies were counted after 24 hr incubation at 37°C. To validate the identity of *C. rodentium,* bacterial colonies were randomly picked and bacterial DNA was purified. The DNA was used to amplify the *eae* gene specific to the DBS100 strain (Petty et al., 2010) by PCR, using the following primers: 5'GCCTCCTGTTGCCTGTAG3' (forward) and 5'CCGATCAGAATGGTTATGC3'(reverse). DNA purified from uninfected mouse feces was used as a negative control.

Microbiota depletion

Mouse intestinal commensal bacteria were depleted using antibiotic-induced microbiota-depleted (AIMD) model as described previously (Mukherji et al., 2013; Rakoff-Nahoum et al., 2004). Mice were treated with a cocktail of antibiotics in drinking water (ampicillin 1g/L; vancomycin 500 mg/L; neomycin sulfate 1g/L; and metronidazole 1g/L, all from Sigma-Aldrich) for 4 weeks before being subjected to *C. rodentium* infection. Controls were treated with regular water. To validate the effectiveness of the antibiotic cocktail in gut bacterial depletion, bacterial DNA was purified from fecal pellets from mice with or without this 4-week antibiotic treatment. The DNA was used to PCR-amplify the bacterial 16S rRNA gene using the universal 16S primers: Eub338-5'ACT CCT ACG GGA GGC AGC AG3' (forward) and Eub518-5'ATT ACC GCG GCT GCT GG3' (reverse) based on published work (Fierer et al., 2005).

Bone marrow transplantation

BM transplantation was carried out based on previously published procedure (Szeto et al., 2012). In brief, recipient $Rag1^{-/-}$ mice (6-week old males) were subjected to lethal γ-irradiation (1050 rads, at 200 rads/min), and 6 hours later the mice were transplanted with donor BM cells ($5x10^{6}$ BM cells/mouse) through retra-orbital injection. The donor BM cells were obtained from

$VDR^{flox/flox}$ or $VDR^{flox/flox}$;RORγt-Cre mice. Eight weeks after transplantation, colonic mucosal LP cells were isolated from the recipient mice and ILC3 populations were analyzed by flow cytometry. To validate the success of BM transplantation, in parallel experiments CD45.1 recipient mice were lethally irradiated and transplanted with CD45.2 donor BM cells. Eight weeks after transplantation, the CD45.1 and CD45.2 cell populations in the blood and colonic lamina propria of the recipients were quantified by FACS analysis.

Vitamin D or vitamin D analog treatment

To study the effect of vitamin D on gut ILC3 development, $Cyp27b1^{-/-}$ mice were treated with $1,25(OH)_2D_3$ (AbbVie) at 300 ng/kg (dissolved in 70% propylene glycol) by daily i.p. injection for one week. In another experiment, WT mice were treated with active vitamin D analog paricalcitol (19-nor-1,25-dihydroxyvitamin D_2, AbbVie) at 300 ng/kg (dissolved in 70% propylene glycol) by daily i.p. injection for one week. Controls were treated with 70% propylene glycol vehicle. These treatments did not raise blood calcium levels as reported previously (Zhang et al., 2008; Zhou et al., 2008). After the treatment, colonic LP cells were isolated and subjected to FACS analyses for ILC3 populations.

Lamina propria (LP) cell preparation

LP cells were isolated from the colon as described previously (Zheng et al., 2008). In brief, mice were killed, and the colons were dissected, cut open longitudinally and washed in cold PBS. The colons were cut into 1.5 cm pieces and washed in PBS containing 1 mM DTT for 10 min at room temperature on a shaker, followed by two washes with shaking in PBS containing 30 mM EDTA and 10 mM HEPES at 37°C for 10 min. The tissues were then digested in RPMI 1640 medium containing DNase I (150 μg/ml, Sigma-Aldrich) and collagenase VIII (150 U/ml, Sigma-Aldrich) with 10% fetal bovine serum at 37°C in a 5% CO_2 incubator for 1.5 hrs. Digested cell suspensions were passed through a 70 μm cell strainer and separated by centrifugation on a discontinuous 40%/80% Percoll gradient at 2500 rpm for 20 min at room temperature. Cells were then harvested for flow cytometric analyses.

Flow cytometry

Flow cytometric analysis was performed as described previously (Shi et al., 2016). Non-specific binding to Fc receptors was blocked with anti-CD16/32 antibody (eBioscience) before cell surface staining. For intracellular staining, cells were fixed and permeablized using a Mouse Regulatory T Cell Staining Kit (eBioscience). For cytokine production, cells were stimulated with PMA (50 ng/ml) and ionomycin (500 ng/ml) for 4 hrs. Brefeldin A (2 μg/ml) was added 2 hrs before cells were harvested for analysis. Dead cells were excluded from the analysis using a Live and Dead Violet Viability Kit (Invitrogen**).** ILC3 was defined as $CD3^-ROR\gamma t^+$, $NKp46^+$ cells as $CD3^-ROR\gamma t^+NKp46^+$, LTi0 cells as $CD3^-ROR\gamma t^+NKp46^-CD4^-$ and LTi4 cells as $CD3^-ROR\gamma t^+NKp46^-CD4^+$. Antibodies used in flow cytometric analyses as follows: anti-CD3e-FITC (clone 145-2C11, Biolegend), anti-CD4-Pecy7 (clone RM4-4, Biolegend), anti-NKp46-Percp-Cy5.5 (clone 29A1.4, Biolegend), anti-RORγt-PE (clone AFKJS-9, eBioscience), anti-IL-22-APC (clone IL22JOP, eBioscience), anti-Ki67-eFluor660 (clone SolA15, eBioscience), anti-CD103-APC (clone 2E7, eBioscience), anti-CD45.1-FITC (clone A20, Biolegend), and anti-CD45.2-PE (clone 104, Biolegend). Cell apoptosis detection with Annexin V-7AAD staining was performed using the Annexin V Apoptosis Detection Kit from BD Biosciences (#559763). Fluorescence-activated cell sorting (FACS) was performed in a BD LSRFortessa unit (BD Biosciences) and data analyzed by FlowJo software V10 (Tree Star Inc).

In vitro ILC3 proliferation

Colonic LP cells were prepared from $Rag1^{-/-}$ mice and Lin^{-}(CD11c, CD11b, CD3, CD19, B220, NK1.1, TER119, Ly6G)$Thy1.2^{hi}KLRG1^{-}IL\text{-}7R\alpha^{+}$ cells were sorted by FACS as described previously (Spencer et al., 2014), using a BD FACSAria Fusion unit (BD Biosciences). These cells were then cultured at $1x10^4$ cells/well in 50 μl RPMI 1640 supplemented with 10% FBS, 1x penicillin/streptomycin, non-essential amino acids, β-mercaptoethanol (50 mM), IL-7 (10 ng/ml, Biolegend) and SCF (10 ng/ml, Biolegend) in the presence or absence of $1,25(OH)_2D_3$ (20 nM). After 3 days of culture, $Ki67^{+}ROR\gamma t^{+}$ cell populations were quantified by FACS analysis. The antibodies used in the sorting were as follows: anti-CD11c-PE (clone N418, eBioscience), anti-CD11b-PE (clone M1/70, Biolegend), anti-CD3-PE (clone 145-2C11, Biolegend), anti-B220-PE (clone RA3-6B2, eBioscience), anti-NK1.1-PE (clone PK136, BD Biosciences), anti-TER119-PE (clone TER-119, eBioscience), anti-Ly6G-PE (clone RB6-8C5, eBioscience), anti-Thy1.2-Pecy7 (CD90.2) (clone 53-2.1, eBioscience), anti-KLRG-PercpCy5.5 (clone 2F1, BD Biosciences), anti-IL-7Rα-efluo660 (CD127) (clone A7R34, eBioscience).

Statistical analysis

Data values were presented as means ± SEM. Statistical comparisons were carried out using unpaired two-tailed Student's *t*-test for two group comparisons, and for three or more group comparisons two-way analysis of variance (ANOVA) was used with a Student-Newman-Keuls post-hoc test. Animal body weight changes and survival rate were analyzed by log-rank test. $P< 0.05$ were considered statistically significant.

Supplemental References

Bouladoux, N., Harrison, O.J., and Belkaid, Y. (2017). The Mouse Model of Infection with Citrobacter rodentium. Curr Protoc Immunol *119*, 19 15 11-19 15 25.

Chen, S., Law, C.S., Grigsby, C.L., Olsen, K., Hong, T.T., Zhang, Y., Yeghiazarians, Y., and Gardner, D.G. (2011). Cardiomyocyte-specific deletion of the vitamin D receptor gene results in cardiac hypertrophy. Circulation *124*, 1838-1847.

Fierer, N., Jackson, J.A., Vilgalys, R., and Jackson, R.B. (2005). Assessment of soil microbial community structure by use of taxon-specific quantitative PCR assays. Appl Environ Microbiol *71*, 4117-4120.

He, L., Liu, T., Shi, Y., Tian, F., Hu, H., Deb, D.K., Chen, Y., Bissonnette, M., and Li, Y.C. (2018). Gut Epithelial Vitamin D Receptor Regulates Microbiota-Dependent Mucosal Inflammation by Suppressing Intestinal Epithelial Cell Apoptosis. Endocrinology *159*, 967-979.

Koroleva, E.P., Halperin, S., Gubernatorova, E.O., Macho-Fernandez, E., Spencer, C.M., and Tumanov, A.V. (2015). Citrobacter rodentium-induced colitis: A robust model to study mucosal immune responses in the gut. J Immunol Methods *421*, 61-72.

Li, Y.C., Amling, M., Pirro, A.E., Priemel, M., Meuse, J., Baron, R., Delling, G., and Demay, M.B. (1998). Normalization of mineral ion homeostasis by dietary means prevents hyperparathyroidism, rickets, and osteomalacia, but not alopecia in vitamin D receptor-ablated mice. Endocrinology *139*, 4391-4396.

Li, Y.C., Pirro, A.E., Amling, M., Delling, G., Baron, R., Bronson, R., and Demay, M.B. (1997). Targeted ablation of the vitamin D receptor: an animal model of vitamin D-dependent rickets type II with alopecia. Proc Natl Acad Sci U S A *94*, 9831-9835.

Mombaerts, P., Iacomini, J., Johnson, R.S., Herrup, K., Tonegawa, S., and Papaioannou, V.E. (1992). RAG-1-deficient mice have no mature B and T lymphocytes. Cell *68*, 869-877.

Mukherji, A., Kobiita, A., Ye, T., and Chambon, P. (2013). Homeostasis in Intestinal Epithelium Is Orchestrated by the Circadian Clock and Microbiota Cues Transduced by TLRs. Cell *153*, 812-827.

Panda, D.K., Miao, D., Tremblay, M.L., Sirois, J., Farookhi, R., Hendy, G.N., and Goltzman, D. (2001). Targeted ablation of the 25-hydroxyvitamin D 1alpha -hydroxylase enzyme: evidence for skeletal, reproductive, and immune dysfunction. Proc Natl Acad Sci U S A *98*, 7498-7503.

Petty, N.K., Bulgin, R., Crepin, V.F., Cerdeno-Tarraga, A.M., Schroeder, G.N., Quail, M.A., Lennard, N., Corton, C., Barron, A., Clark, L., et al. (2010). The Citrobacter rodentium genome sequence reveals convergent evolution with human pathogenic Escherichia coli. J Bacteriol *192*, 525-538.

Rakoff-Nahoum, S., Paglino, J., Eslami-Varzaneh, F., Edberg, S., and Medzhitov, R. (2004). Recognition of commensal microflora by toll-like receptors is required for intestinal homeostasis. Cell *118*, 229-241.

Shi, Y., Liu, T., He, L., Dougherty, U., Chen, L., Adhikari, S., Alpert, L., Zhou, G., Liu, W., Wang, J., et al. (2016). Activation of the Renin-Angiotensin System Promotes Colitis Development. Sci Rep *6*, 27552.

Spencer, S.P., Wilhelm, C., Yang, Q., Hall, J.A., Bouladoux, N., Boyd, A., Nutman, T.B., Urban, J.F., Jr., Wang, J., Ramalingam, T.R., et al. (2014). Adaptation of innate lymphoid cells to a micronutrient deficiency promotes type 2 barrier immunity. Science *343*, 432-437.

Szeto, F.L., Reardon, C.A., Yoon, D., Wang, Y., Wong, K.E., Chen, Y., Kong, J., Liu, S.Q., Thadhani, R., Getz, G.S., et al. (2012). Vitamin D receptor signaling inhibits atherosclerosis in mice. Mol Endocrinol *26*, 1091-1101.

Zhang, Z., Zhang, Y., Ning, G., Deb, D.K., Kong, J., and Li, Y.C. (2008). Combination therapy with AT1 blocker and vitamin D analog markedly ameliorates diabetic nephropathy: blockade of compensatory renin increase. Proc Natl Acad Sci U S A *105*, 15896-15901.

Zheng, Y., Valdez, P.A., Danilenko, D.M., Hu, Y., Sa, S.M., Gong, Q., Abbas, A.R., Modrusan, Z., Ghilardi, N., de Sauvage, F.J., et al. (2008). Interleukin-22 mediates early host defense against attaching and effacing bacterial pathogens. Nature medicine *14*, 282-289.

Zhou, C., Lu, F., Cao, K., Xu, D., Goltzman, D., and Miao, D. (2008). Calcium-independent and 1,25(OH)2D3-dependent regulation of the renin-angiotensin system in 1alpha-hydroxylase knockout mice. Kidney Int *74*, 170-179.